Journal of Oil Palm Research Vol. 14 No.1, *June* 2002, p. 35-44

MICROSTRUCTURE OF MEDIUM DENSITY FIBREBOARD FROM OIL PALM EMPTY FRUIT BUNCH FIBRE

RIDZUAN RAMLI*; STEPHEN SHALER and MOHD ARIFF JAMALUDIN+**

ABSTRACT

Using sequentially acquired 2-D *images of microtome sections via* a *light microscope,* 3-D *models of the microstructure of commercial and laboratory produced medium density fibreboards (MDF) were constructed. To assess the accuracy of the* 3-D *models, they were analysed for their ratios of inter-fibre void using an image analysis technique. The study indicated that* it *was feasible to use this technique to determine the variation in inter-fibre void ratio* at *different depths in the* MDF. *The ratio of void area varied significantly in* a *gradient from the top/bottom of the boards to the core (middle). However, in the other directions (along the length and breadth), there were no significant differences in the void ratio. The ratio of void area within each panel was negatively related to the density.*

Keywords: image analysis, medium density fibreboard, 2-D image, 3-D models, three-dimensional reconstruction.

INTRODUCTION

Knowledge of the internal structure of wood and wood-based materials is important *for* understanding their structural properties. This is normally obtained by microscopic examination but conventional optical microscopy is only one of many techniques used in wood science. In most of the techniques, with the exception of the recently introduced laser scanning confocal microscopy, the information is painstakingly compiled *from* two-dimensional images (Jang et al., 1991). However, even with the rather expensive laser microscopy, thick non-transparent objects, such as MDF, are difficult to visualize. Thus, modelling remains in vogue, especially the improved methods of 3-D construction *from* serial 2-D images of microscopic sections.

Image analysis by the manipulation of two-dimensional images is finding increasing applications in wood science (Choi *et al.*, 1991; Ellis *et al.*, 1994; Lau and Tardiff, 1990; McMillin, 1982; Miller *et al.*, 1973). Faster computers, coupled with better image analysis techniques, have enabled more and more detail to be captured *from* the images, obviating the time consuming stereological methods.

A considerable volume of wood composites is air space, or void, *from* the random deposition of fibre in their production. Although the voids are greatly reduced by the compression used in producing the composites, a sufficient volume remains to influence the physical and mechanical properties of the products. Therefore, knowledge of the size, orientation and frequency of the voids is important *for* a better understanding of the composite behaviour.

Many techniques have been used to study the spatial structure of wood composites, including electro osmotic techniques *for* measuring pore size (Hosli, 1981) and mercury porosimetery to determine total porosity, density and pore size distribution (Blakenhorn et al, 1978; Dai and Stener, 1994). Kallmess et *al.* (1961) developed theoretical models to predict the fibre (flake) length, coverage and void size *from* simulated randomly formed networks.

Recently, Donaldson and Lomax (1989) and Murmanis et *al.* (1986) used microscopy to study MDF. Subsequently, Ellis et al. (1994) constructed 3-D models *from* 2-D images obtained *from* the direct scanning of orientated strand board (OSB).

* Malaysian Palm Oil Board, P.O. Box 10620, 50720 Kuala Lumpur, Malaysia.
** Faculty of Wood Science, University of Maine, Orono, USA.
+ Faculty of Forestry, Universiti Putra Malaysia, 43400 UPM Serdang, Selangor, Malaysia.

The construction of 3-D images in biomedical studies was discussed by *Blakenhornet aI.* (1978) and Farrell and Zappulla (1989). Most of the methods in 3-D construction use expensive equipment in a process which typically requires the complicated registration of images in sequence. With the development of confocal microscopes and computerized axial tomography, volume modelling of materials from 2-D images has improved greatly (Montgomery and Muriel, 1993).

In this study, a 3-D solid VOXEL (volume pixels) microstructure of MDF was constructed from 2-D images of a series of resin-embedded microscopic sections captured with a light microscope. The objective was to assess the potential of this technique for modelling the structure of a MDF panel throughout its volume in all three directions - *x* (breadth, b), *Y* (length, 1) and z (height, h) *(Figure* 1) by using the model to estimate the inter-fibre void ratio in MDF panels.

METHODS AND MATERIALS

Two types of MDF were used - commercial Douglas fir *(Pseudotsuaga* spp.) and laboratory-produced boards – each with three panels. With reference to *Figure* 1, a block of 24 mm (b) x 40 mm (1) x 12 mm (h) was cut from each panel. Each block was then cut at 4 mm intervals along their band 1 so that 60 sub-blocks of 4 mm x 4 mm x 12 mm were obtained. In the sub-blocks, the 1 of 12 mm therefore represented the h of the previous blocks.

To model the structural changes along the z-direction (h) of the blocks, 10 sub-blocks were randomly taken per block, five each from both ends (lengthwise) of a block. As there were three boards for each type of MDF, 30 sub-blocks were taken per type of MDF. Out of the 30, 10 samples were randomly picked and cut across their 1 (or across the h of the original blocks) into cubes of 4 mm x 4 mm x 4 mm, representing the top, middle (or core) and bottom sections of the blocks. Ten of the cubes were then picked [randomly except for equal numbers from the top /bottom (which should be similar) and middle sections for sectioning].

To model the structure along the x-direction (1), five sub-blocks per panel were taken at random along its 1. They were then cut into cubes as above, and two and three taken from the top /bottom and core of the original blocks, respectively, or *vice versa.*

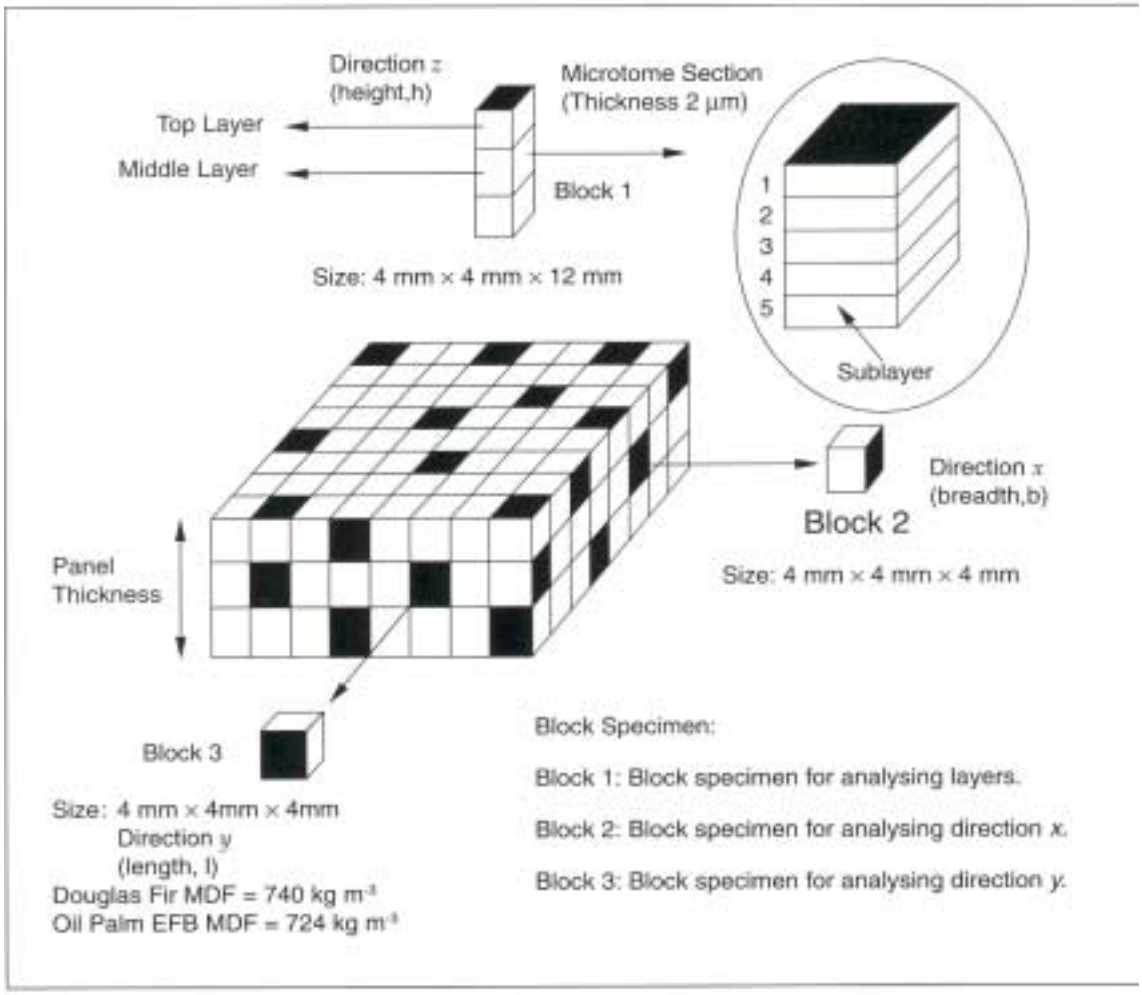

Figure 1. Illustration af sample preparation.

From the three panels for each type of MDF, therefore, 15 cubes were taken, either seven from the top /bottom and eight from the core, or *vice versa*. To model the structure along the y-direction (b), the same procedure was adopted as for the x-direction (1) except that the sub-blocks were taken along the b. The numbers of cubes taken for the different

TABLE 1. IMAGING SAMPLES TAKEN FROM EACH TYPE OF BOARD

Species	MDF
No. of boards	3
1) Block for direction - z	
Total No. of blocks	3 x 10 = 30
No. of randomly selected blocks	10
Total No. of sections for imaging	5 x 10 = 50
2) Block for direction - *y*	
Total No. of blocks	3 x 5 = 15
No. of randomly selected blocks	3
Total No. of sections (sub-layers)	5 x 3 = 15
3) Block for direction -*x*	
Total No. of blocks	5 x 3 = 15
No. of randomly selected blocks	3
Total No. of sections (sub-layers)	3 x 5 = 15

directions are shown in *Table* 1.

The cubes were conditioned in a humidity chamber for 24 hr (55% RH, 22°C), trimmed and embedded in resin following the techniques of Mollenhauer (1964). The technique involved a five-stage solvent exchange (dehydration with 50% to 100% ethanol) followed by embedment in DDSA (11 ml), Epon 812 (5.2 ml), Araldite 506 epoxy resin (8.1 ml), dibutyl phthalate (0.75 ml) and DMP 30 (26 drops). Before adding the DMP 30, the resin mixture was allowed to mix thoroughly for 5 min. The cubes were placed in standard flat silicon embedding moulds, and the moulds then filled with the embedding resin. The resin-embedded cubes (moulds) were then placed in an oven at 45°C to 50°C for 48 hr until polymerization of the resin was complete.

The hardened (polymerized) cubes were then trimmed using a razor to a rhomboid shape with smooth surfaces. Using a water-immersed ultra microtome, 5 x 2.0 μm thick sections were cut, each representing a sub-layer. During the sectioning, the correct water level was always maintained in the knife trough to avoid damaging the section void areas. The direction of sectioning for each cube was across its axis of interest, *e.g.* for studying the variation with h, the cubes were transversely sectioned across the z-direction.

All the five sections from a cube were carefully transferred to pre-cleaned microscopic slides, with the sequence carefully recorded, and affixed with the same resin formulation used in the embedding. Each slide was marked to identify the direction for which it was sliced *(x, y* or z) and placed on a hot plate at 80°C until dry to the touch. The dried sections were then stained (with 1 % toluene blue and 1% sodium borate), re-dried on the same hot plate and rinsed with distilled water before final drying and covering with a glass slip.

Image Analysis

The image acquisition system used consisted of a light microscope, CCD video camera, PC and PC frame grabber (Anon., 1995) with 320 x 240 pixels resolution and eight monochrome bits per pixel.

From each microscopic slide, a section of the rhomboid of approximately 1.5 mm x 1.5 mm was captured at x100 magnification through the CCD video camera. Within this area, a smaller area of interest (AOI) of approximately 1.32 mm2 was identified and its image acquired and saved in tagged image file format (TIFF). The images from the five layers of each cube were saved sequentially so that their AOIs could be visually imposed on each other, from the top downwards.

Software calibration (Anon., 1993) was performed using a reticule slide. Each image was enhanced for contrast between the void area (light) and solid material (dark). The enhancement was performed using the Look-Up Table method for remapping the pixel intensity values to the entire 0 - 255 range *(Figures 2a* and *2b).*

The inter-fibre voids (not the intra-fibre voids) were then darkened by manually assigning their pixels the maximum value of 255. Each of the areas was automatically measured *(Figure* 3) and the total area obtained. The percentage of void area was calculated using Equation 1 *(Figure* 4).

$$\% \text{ Inter-fibre void} = \frac{\text{sum of inter-fibre void area in AOI} \times 100}{\text{AOI}} \quad [1]$$

The measured percentage inter-fibre void was then compared to the theoretical void volume ratio calculated from Equation 2 (Siau, 1984). The specific gravity of the woody raw material of the MDF was assumed to be 1.5 corresponding to a specific volume of 0.667 cm3 g-l. In using the formula, the effect of the resin on the product density / porosity relation was assumed to be negligible.

$$Va = 1 - G\,(0.667 + 0.01\,M) \quad [2]$$

where:

Va = porosity, or fractional void volume of MDF.
G = density of MDF (from y- ray densitometer).
M = moisture content of the panel (assumed to be 6%).

Figure 2a. *Typical initial captured image.*

Figure 2b. *Enhanced image resulting from look-up table operation.*

Figure 3. *Illustration showing the void area measured by flooding with overlay layers.*

Three-dimensional Construction

The enhanced 2-D images from the five layers were transformed into a 3-D solid volume model *of* the cube using commercial software, Spyglass Slicer (Anon., 1994). From the model, slices could be rendered in orthogonal planes, or any arbitrary angle, and iso-surfaces created for specific intensity values. The stacking into solid voxel's was accomplished by discretizing all the sections saved in sequence in a sub-cube *of* 0.66 x 0.66 x 0.66 mm3 (290 x 290 x 290 cu. pixel) dimensions and interpolating the elemental concentrations in-between the layers. The stacked images were kept equal in area *to* enable this process. In this study, all the images had an AOI *of* 1.32 mm2.

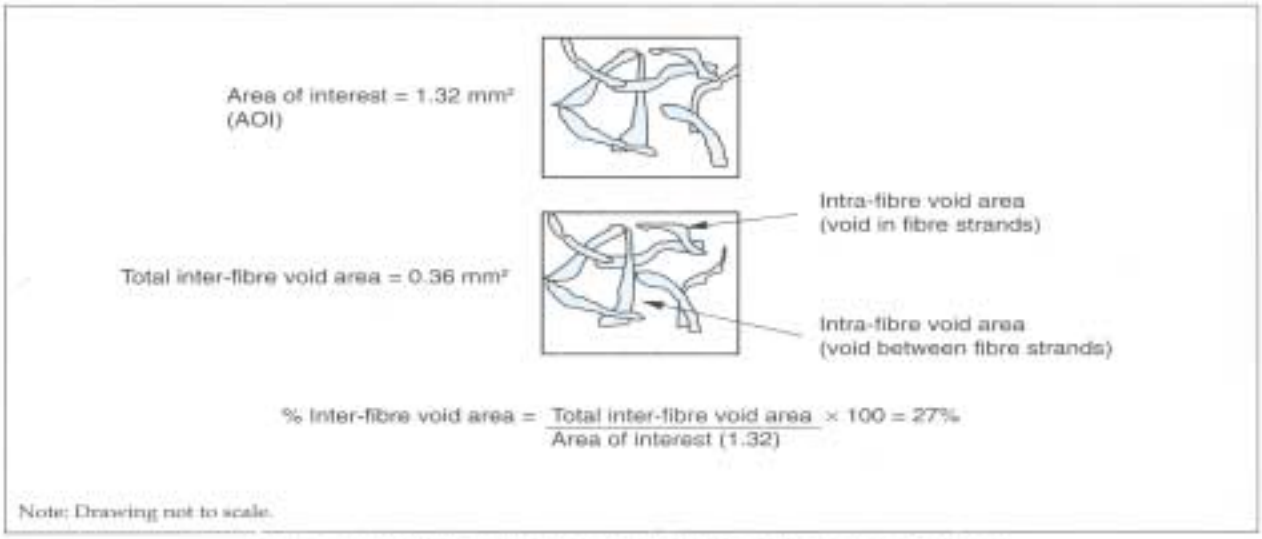

Figure 4. Calculation of percentage inter-fibre void area in captured AOI image.

Statistical Analysis of the Inter-fibre Void Area

Prior to data analysis, all the areas of the individual inter-fibre voids were transformed into A-sin square root values to normalize the distribution as shown in *Figures Sa* and *Sb.*

The first set of data was along the z-direction, or height. It showed the variation in inter-fibre void ratio from the surface (top or bottom) to the core of the panel, as well as through the layers within the sub-cubes (nested two-way ANOVA). The subsequent data sets were for the variation along the *x*- and y-directions.

RESULTS AND DISCUSSION

Variation in Inter-fibre Void Ratio between Layers

The average inter-fibre void ratios and a summary for the nested two-way ANOV A are given in *Tables* 2 and 3, respectively. The ratio in the core was significantly higher ($P > 0.01$) than in the surface for both the types of MDF as the density decreased from the surface inwards (Laufenberg, 1986; Ridzuan, 1995; Suchland and Woodson, 1986). The average measured void ratios for all the panels were lower than their theoretical ratios because the equation by

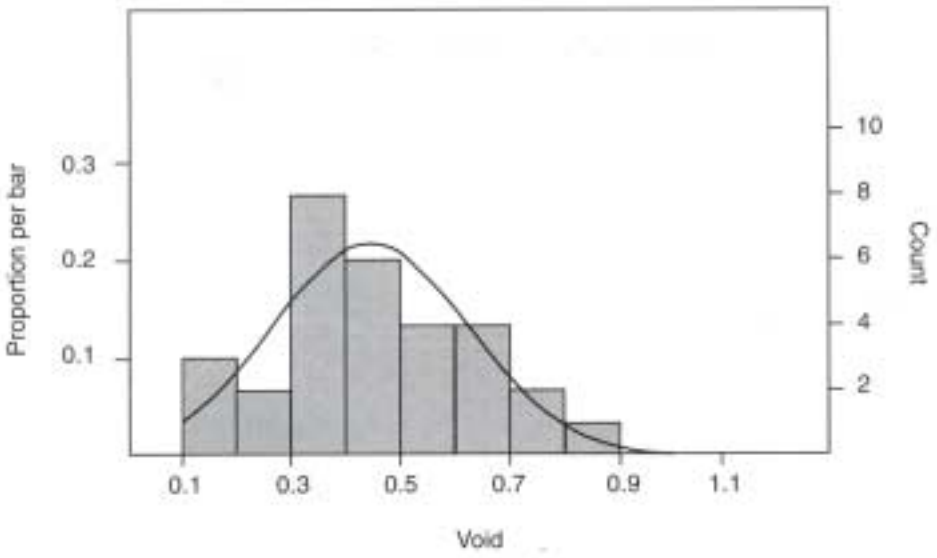

Figure 5a. Untransformed data on inter-fibre void ratio.

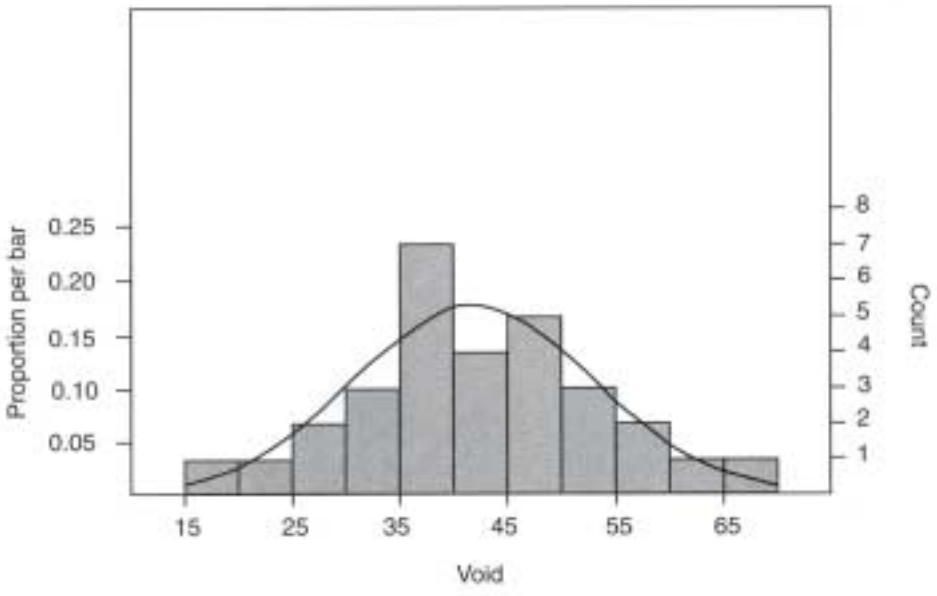

Figure 5b. Transformed data [to Asin (Sqrt)] on inter-fibre void ratio.

TABLE 2. AVERAGE INTER-FIBRE VOID RATIOS AND CALCULATED DENSITIES

	Surface layer			Core layer		
	Inter-fibre ratio measured (%)	Inter-fibre ratio calc. (%)	Density g cm^{-3} [a]	Inter- fibre ratio measured (%)	Inter-fibre ratio calc. (%)	Density g cm^{-3} [a]
MDF [d]	31.2(2.491)[b] [25][c]	37.2	0.940 (0.017) [6]	39.7 (4.411) [25]	54.9	0.674 (0.010) [3]
MDF EFB	31.9(3.405) [25]	41.2	0.880 (0.023) [6]	39.7(4.191) [25]	54.2	0.685 (0.014) [3]

Notes:
[a] Density from direct gamma-ray scanning.
[b] Standard deviation.
[c] Number of samples.
[d] Commercial MDF.

TABLE 3. ANOVA OF VOID RATIOS BETWEEN LAYERS IN COMMERCIAL AND OIL PALM EMPTY FRUIT BUNCH MEDIUM DENSITY FIBREBOARD

Source	Sum of squares	DF	Mean square	F-ratio	P-value
Panel type	3.223	1	3.223	0.239	0.626
Layers	1 645.049	1	1 645.049	121.824	0.000**
Panel type * layers	127.435	8	15.929	1.180	0.320
Sub-layers (layers)	3.145	1	3.145	0.233	0.631
Error	1 188.302	88	13.503	-	-

Note: ** Highly significant at 0.01 level.

Siau (1984) accounted for all the voids in wood. MDF, however, is impregnated with resin and compressed, both of which operations reduced the voids.

Figures 6a and *6b* show typical images across the z-direction for the laboratory and commercial MDF panels, respectively. The lighter regions represent the voids while the fibre (solid material) is darker, making its predominant orientation readily apparent.

The summary results for ANOVA in *Table* 3 indicate that the MDF type, interaction between the two factors (panel type and layers) and sub-layers (the five microtome sections from a cube) within layers (top / bottom or middle) were not significantly different in void ratio.

Table 4 presents the average inter-fibre void ratios along the *x*- and y-directions, and *Table* 5 the summaries of the one-way ANOVA. For a given panel type, the ratio of inter-fibre void did not differ between the two directions (a = 0.05). *Figures 7a* to 7 *d* are the images from transverse-sections along the *x*- and y-directions illustrating the randomness of the fibre orientation and the voids in both the types of boards.

The statistical summaries in *Tables* 6 and 7 show the variation in void area of the MDF from seven

Figure 6a. Image of an empty fruit bunch laboratory panel along the z-direction (transverse section perpendicular to the height).

Figure 6b. Image of commercial medium density fibreboard panel along the direction (transverse section perpendicular to the height).

TABLE 4. AVERAGE VOID RATIOS PARALLEL TO THE EDGES OF PANELS IN *x*- AND *y*-DIRECTIONS

	x-section	*y*-section
	Inter-fibre ratio measured (%)	Inter-fibre ratio calculated (%)
MDF[c]	47.94	38.31
	(18.47)[a]	(9.63)
	[15][b]	[15]
EFB	44.41	39.33
	(12.42)	(9.78)
	[15]	[15]

Notes:
[a] Standard deviation.
[b] Number of samples.
[c] Commercial MDF.

calibrations and the remapping of five images, respectively. The small coefficients of variance (COY) in both the tables suggest that the calibration precision and image enhancement were not significant sources of error in the inter-fibre void determinations. There was no correlation between the mean void size and COY as influenced by the different remapping values.

The overall error induced by the different levels of image enhancement (threshold level), precision in calibration and the repeatability of the technique applied did not affect the measurements of the void area. The potential operator errors in the preparation of slides (embedding, sectioning, staining and

TABLE 5. ANOVA OF VOID RATIOS PARALLEL TO THE EDGES OF PANELS IN *x*- AND *y*-DIRECTIONS IN COMMERCIAL AND EMPTY FRUIT BUNCH MEDIUM DENSITY FIBREBOARD

Square	Sum of squares	DF	Mean square	F-ratio	P-value
A. MDF EFB					
Direction	193.747	1	193.747	1.550	0.223
Error	3 499.933	28	124.998	-	-
B. MDF[a]					
Direction	696.525	1	696.525	3.210	0.084
Error	6 075.946	28	216.998	-	-

Note: [a] Commercial MDF.

Figure 7 a. Image of an empty fruit bunch laboratory panel along the x-direction (transverse section perpendicular to the breadth).

Figure 7b. Image of an empty fruit bunch laboratory panel along the y-direction (transverse section perpendicular to the length).

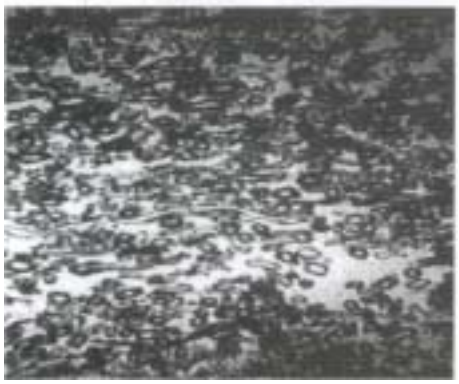

Figure 7 c. Image of commercial medium density fibreboard panel along the x-direction (transverse section perpendicular to the breadth).

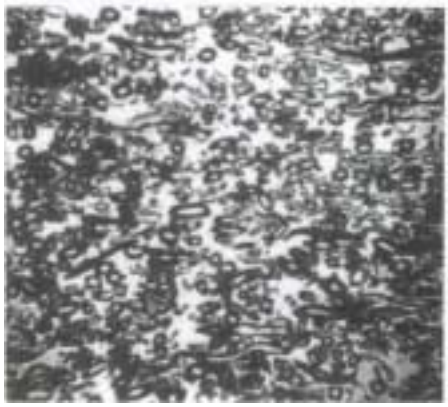

Figure 7d. Image of commercial medium density fibreboard panel along the y-direction (transverse section perpendicular to the length).

TABLE 6. EFFECT OF CALIBRATION PRECISION ON MEASUREMENT OF VOID AREA (accuracy of calibration)

Number of calibrations	7
Mean (mm^2)	0.398
Standard deviation (mm^2)	0.006
Standard error	0.002
Coefficient of variation (%)	1.5

especially in the z-direction (h or thickness). This was mainly because only five images were used to construct a model. The limited number of images, with discrete differences between themselves, was not sufficient to eliminate all the background *noises* (blurs) and uneven illumination captured during acquisition of the 2-D images, reducing the sharpness of the 3-D models.

TABLE 7. EFFECT OF IMAGE REMAPPING AT DIFFERENT LEVELS OF INTENSITY (image enhancement) ON MEASUREMENT OF VOID AREA

Void	Void 1	Void 2	Void 3	Void 4	Void 5
Number of intensity levels	5	5	5	5	5
Mean void size (mm^2)	9.45E-6	1.67E-5	1.35E-6	2.48E-5	1.26E-5
Standard deviation (mm^2)	0.000	0.000	5.68E-8	1.06E-5	3.27E-7
Standard error	0.000	0.000	2.32E-8	4.33E-7	1.33E-7
Coefficient of variation (%)	0.000	0.000	4.2	4.3	2.6

mounting) are unlikely to be important because of the consistent technique used.

Three-dimensional Construction

A solid voxel model was constructed *(Figure* 8) using a commercial software (Anon., 1994) from the series of 2-D images taken from the five layers in a cube. From this model, various views could be obtained through orthogonal slicing (perpendicular to the *x*-, *y*- or z-axis) and/or arbitrarily-oriented diagonal slicing as shown in *Figure* 9. Another technique possible was to *cut* 2-D slices from the 3-D model as shown in *Figure* 10. From the images *sliced,* the internal structure of the material can be discerned and related to its properties.

Although 3-D models were successfully generated from 2-D images, the voxel was fairly crude,

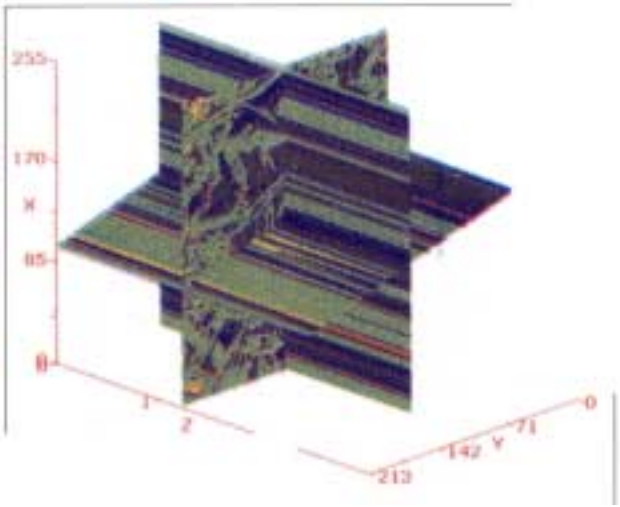

Figure 9. *Slices rendered in orthogonal planes (x, y, z) and arbitrary angles.*

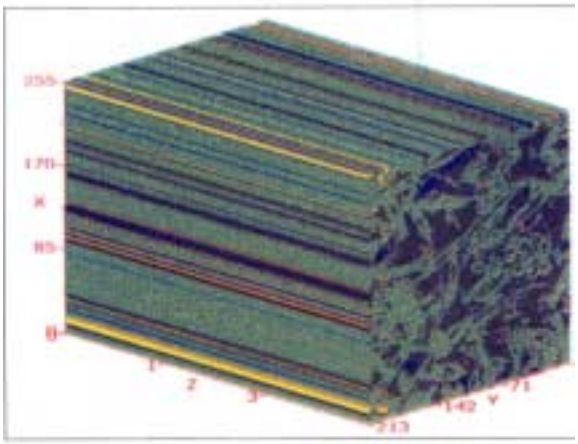

Figure 8. *A cubic 3-D solid voxel (290* x *290* x *290 cu. pixels) model constructed from 2-D images.*

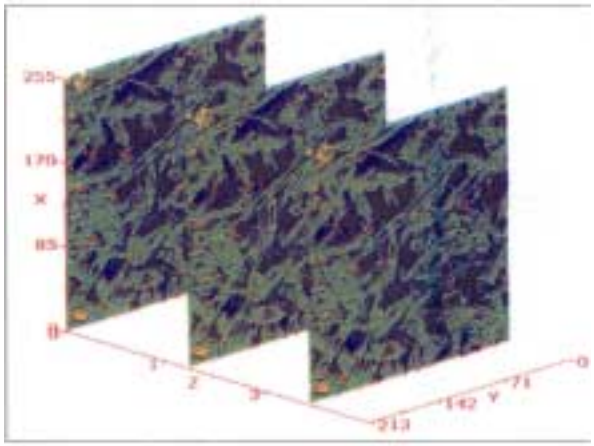

Figure 10. The 2-D slices rendered from a 3-D voxel (290 x *290* x *290 cu. pixels) model.*

However, the poor models were not important, as this work was only to test the methodology. For better models, more images can just be used. In addition, the generation techniques, or interpolation (realignment) between the images, can be improved. Future research will focus on improving the alignment of the images, perhaps borrowing from the method of Marschallinger and Hock (1993). A challenge in using this method for MDF is ascertaining the calibration points. The noises and other biases in image capturing need to be reduced by using signal processing methods.

CONCLUSION

The imaging technique was successfully used to develop 3-D models of MDF panels from 2-D images. The accuracy of the models was assessed by using them to estimate the inter-fibre void volumes in commercial Douglas fir and laboratory-prepared panels. Although the volumes measured were less than those calculated, they were consistent between the two types of MDF. As the void volumes are similar between MDF panels (as attested to by the equally consistent, although higher, calculated values), the consistency of the results suggests that the technique was reliable.

The models obtained were fairly crude but this was not so much a fault of the technique but the extremely limited number of images used to simplify this assessment. More detailed and accurate models can easily be obtained by increasing the number of images. The technique was easy to use and its extreme usefulness in allowing the models developed to be manipulated for detailed study of the internal structure of the material commends its more widespread application in wood science.

ACKNOWLEDGEMENTS

The authors wish to thank those who were directly and indirectly involved in this project. The authors would also like to thank Dr Ma Ah Ngan for his invaluable comments. Appreciation is also given to the Director-General of MPOB for permission to publish this paper.

REFERENCES

ANON. (1993). Sigma Scan Software, 1993. Jandel Scientific, P.O. Box 7005, San 94912-8920, USA.

ANON. (1994). Slicer Software, 1994. Spyglass.Inc., 1230 East Diehl Road, Suite 304 Waterville, Illinois 60563 USA.

ANON. (1995). Snappy Video Snapshot (frame grabber). Play Incorporated, 2890 Kilgore Road, Rancho Cordova, California 95670-6133, USA.

BLAKENHORN, P R; BARNES, D P; KLINE, D, E and MURPHEY, W K (1978). Porosity and pore size distribution of black cherry carbonized in an inert atmosphere. *Wood Sci.,* 11(1): 23-29.

CHOI, D; THORPE, J L and HANNA, R B *(199J).* Image analysis to measure strain in wood and paper. *Wood Sci. Tech.,* 25: 251-26.

DAI and STENER, 1'R (1994). Spatial structure of wood composites in relation to processing and performance characteristics. Part 3. Modeling the formation of multi-layered random flake mats. *Wood Sci. and Tech.,* 28: 229-239.

DONALDSON, L A and LOMAX, T D (1989). Adhesive / fibre interaction in medium density fibreboard. *Wood Sci. Tech.,* 23: 371-380.

ELLIS, S; DUBOIS, J and A VRAMIDIS, S (1994). Determination of parallam macroporosity by optical techniques. *Wood and Fibre Science,* 26(1): 70-77.

FARRELL, E J and ZAPPULLA, R A (1989). Three-dimensional data visualization and biomedical applications. *CRC Critical Reviews in Biomedical* Engineering, 16(4): 323-363.

HOSLI, J P (1981). Determining pore size in wood by electroosmotic measurements. *Wood Sci., 14(2):* 9194.

JANG, H F; ROBERTSON, A G and SETH, R S (1991). Optical sectioning of pulp fibres with confocal scanning laser microscopy. *Tappi Proc. of the* 1991 *International Paper Physics Conference.* p. 277-280.

KALLMES, 0; CORTE, H and BERNIER, G (1961). The structure of paper. II. The statistical geometry of a multiplanar fibre network. *TAPPI.,* 44(7): 519528.

LAU, P W C and TARDIFF, Y (1990). A computeraided image analysis system for analysing cracks created by nailing in wood. J. *Testing Eval.,* 18(2): 131137.

LAUFENBERG, T L (1986). Using gamma radiation to measure density gradients in reconstituted wood products. *Forest Product Journal,* 36(2): 59-62.

MARSCALLINGER, V and HOCK (1993). A method for the 3-D reconstruction of chemically zoned minerals from microprobe scanned serial sections. *USA Microscopic and Analysis,* 11: 13-15.

McMILLIN, C W (1982). Application of automatic image analysis to wood science. *Wood Science,* 14(3): 97-105.

MILLER, D G; TARDIFF, Y and BERGIN, E G (1973). Video wood-failure evaluator. *Forest Product Journal*, 23(4): 21-26.

MOLLENHAUER, H H (1964). Plastic embedding mixtures for use in electron microscopy. *Stain Technol.*, 39: 111.

MONTGOMERY, K and MURIEL, D R (1993). A method for semi-automated serial section reconstruction and visualization of neural tissue from TEM images. Biocomp.arc.nasa.gov / papers / spie_paper.93.html

MURMANIS, L; YOUNGQUIST, J A and MYERS, G C (1986). Electron microscopy study of hard panels. *Wood and Fibre Science*, 18(3): 1-7.

RIDZUAN, R (1995). Properties of medium density fibreboard manufactured from oil palm empty fruit bunches fibres. M. Sc. thesis. University of Maine, Orono.

SIAU, J F (1984). *Transport Processes in Wood.* Sprigler Verlag, Berlin. 29 pp.

SUCHSLAND, O and WOODSON, G E (1986). Fibrepanel manufacturing practices in the United States. USDA Forest Services. *Agri. Handbook No.* 640.